Validation of Shock Calculations in IFCI 6.0
Letter Report

Prepared by

A. W. Reed and M. F. Young
Nuclear Energy Technology Center
Sandia National Laboratories

Prepared for
Division of Systems Research
Office of Nuclear Regulatory Research
U. S. Nuclear Regulatory Commission
Washington, D. C. 20555

NRC JCN W6265

November 14, 1996

1. Introduction

As part of the IFCI assessment process, the shock-predicting capability was tested. This was accomplished by deriving several closed form solutions for a simple 1-D shock, and comparing them to the predictions of IFCI. A closed cylinder 0.8 m long with an inflow condition at the top was used as the configuration for this benchmark. Figure 1 shows a shock propagating in this cylinder (rotated 90°) along the length. In front of the shock, the initial conditions are given by pressure (P_1) and steam density (r_1) at rest (V=0). Behind the shock, the pressure is given by P_2 and ρ_2 at a material velocity V_m. The shock velocity is shown as V_s.

At the start of the IFCI calculation, the volume of the cylinder is described by the pre-shock conditions P_1 and r_1. The inflow conditions are set to the shock conditions (*i.e.* P_2, r_2, V_m). The material velocity, V_m, and the shock velocity, V_s, are calculated from the closed form solution given P_1, P_2, and r_1.

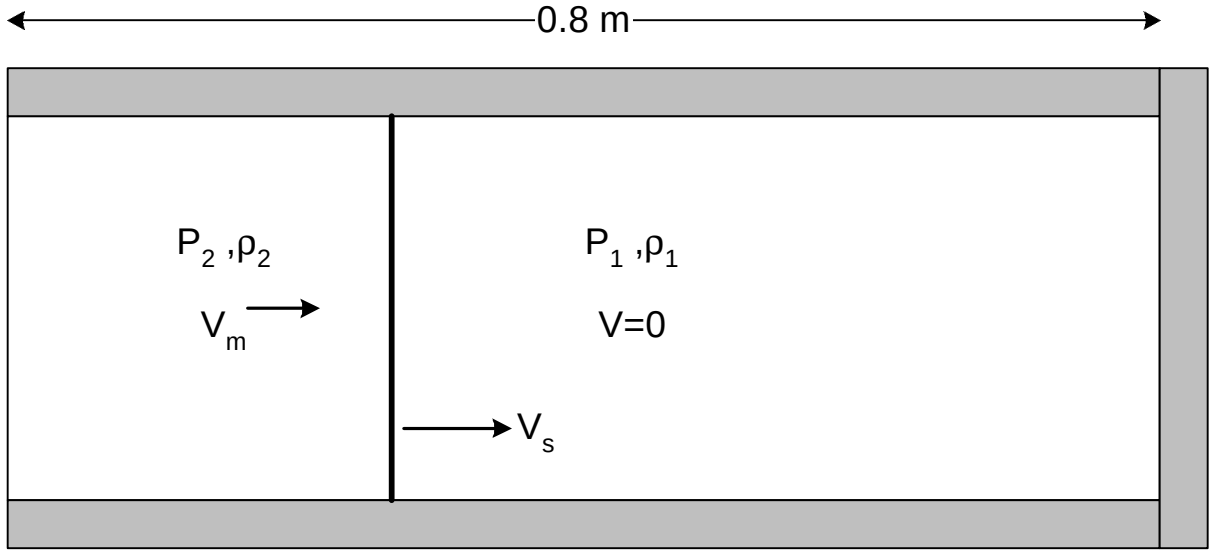

Figure 1 Geometry Used for Shock Benchmark (rotated 90°)

2. Shock Propagation in Water

The first shock to be analyzed is that of a shock wave traveling through solid water. For the case considered here, the shock is isentropic. The shock speed is the acoustic speed, and the temperature and density in the shock region are equal to the temperature and density in the region preceding the shock. The equations for the shock speed, V_s, and the material speed, V_m, are [1]

$$V_s = \sqrt{\frac{1}{r\ b}}$$

$$V_m = \frac{P_2 - P_1}{r\ V_s}$$

where b is the isothermal compressibility, defined by the equation

$$b = -r\ \frac{\P}{\P P}\left(\frac{1}{r}\right)_T .$$

For this calculation, the water temperature was set to 373 K and the pressures P_1 and P_2 were set to 10^5 Pa and 10^6 Pa, respectively. According to the steam tables published by the National Bureau of Standards [2], the acoustic velocity at 100 ^{o}C and 5 MPa is 1542.6 m/s. This implies an isothermal compressibility (b) of $4.384 \bullet 10^{10}$ Pa^{-1}. However, the density change between P_1 and P_2 calculated by IFCI implies a value of $4.934 \bullet 10^{10}$ Pa^{-1}. This is an accurate reflection of the fitting function for the water density transcribed from the TRAC code.[3] Based upon the IFCI-calculated densities, the shock and material velocities should be 1454.3 m/sec and 0.646 m/sec, respectively.

The predicted pressure profiles for the shock are shown in Figure 2. The propagating shock is shown advancing at times of 0.1, 0.2, 0.3, 0.4, and 0.5 ms. The reflected shock is shown for times of 0.6, 0.7, 0.8, and 0.9 ms. The pressure level of the reflected shock compares favorably to the theoretical value of 1.9 MPa.

The velocity of the shock can be determined by tracking the advance of an isobar. Figure 3 shows the positions of the 0.8 MPa and 1.7 MPa isobars, as calculated by IFCI. The slopes of these lines produce shock speeds of 1450 m/s and 1446 m/s for the propagation and reflection waves, respectively. These values compare favorably to the calculated value for the shock

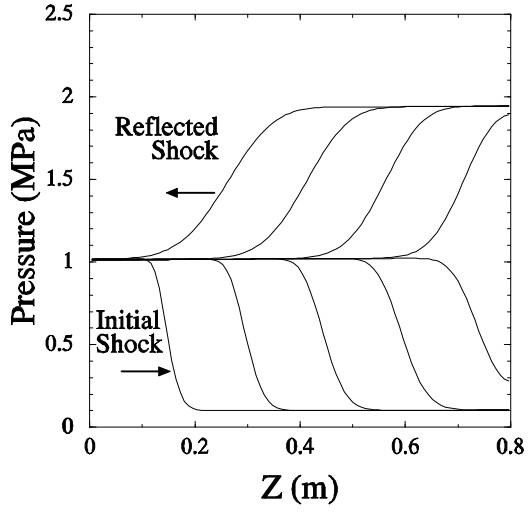

Figure 2 Propagation of Shock and Reflection in Water

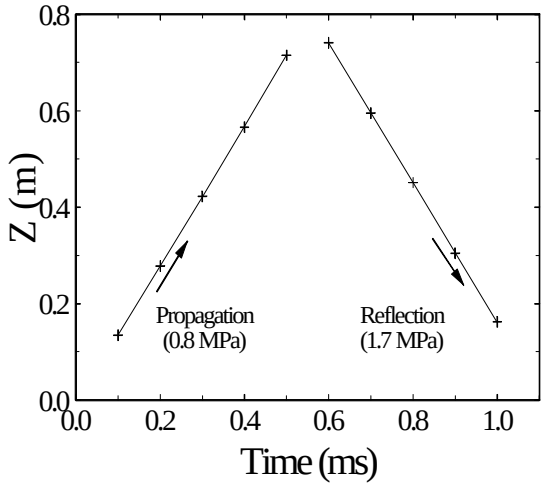

Figure 3 Position of Isobar as a Function of Time (Water Shock)

speed. The lack of variations in the shock pressure and the shock speed indicates that the IFCI calculations are consistent with the closed form solution.

3. Shock Propagation in Steam

The calculation of shocks in highly compressible media requires that the energy equation be included with the continuity and momentum equations.

$$T_1 + \frac{V_s^2}{2\,C_P} = T_2 + \frac{\left(V_s - V_m\right)^2}{2\,C_P}$$

$$P_1 - P_2 = r_1\,V_s\left[\left(V_s - V_m\right) - V_s\right]$$

$$r_1\,V_s = r_2\left(V_s - V_m\right)$$

These equations are solved for the shock velocity (V_s), material velocity (V_m), and shock gas temperature (T_2).

$$V_s = \sqrt{\frac{\left(P_2 - P_1\right) - \dfrac{\left(P_2 - P_1\right)^2}{2\,C_p\;r_1\;T_1}\left(\dfrac{P_1}{P_2}\right)}{r_1\left(1 - \dfrac{P_1}{P_2}\right) - \dfrac{\left(P_2 - P_1\right)}{C_p T_1}\left(\dfrac{P_1}{P_2}\right)}}$$

$$V_m = \frac{\left(P_2 - P_1\right)}{r_1\,V_s}$$

$$T_2 = T_1 + \frac{V_s^2 - \left(V_s - V_m\right)^2}{2\,C_p}$$

The formulation of the energy equation implies a constant specific heat. In order to realize this approximation, a smaller pressure rise was used for this benchmark than was used for the water shock benchmark. The shock pressure was set to 0.2 MPa. The pressure and temperature in the pre-shock region were set to 0.1 MPa and 673 K, respectively. Based on these initial conditions, the shock and material velocities are predicted to be 867 m/s and 358 m/s, respectively. The temperature behind the shock front is predicted to be 790 K.

For highly compressible fluids, the reflected shock characteristics are significantly different than the initial propagating shock. The continuity, momentum, and energy equations are the same as for the initial propagating shock, with the exception that the thermodynamic state of the fluid feeding into the reflected shock is determined by the initial propagation (i.e. r_2, T_2, P_2, V_m). In order to satisfy the boundary condition at the reflecting surface, the material velocity behind the reflected shock must be zero. The equations for the reflected shock velocity (V_{sr}), pressure (P_3), and temperature (T_3) are:

$$V_{sr} = \frac{-\left[\frac{V_m}{2}\left(\frac{2\, r_2\, T_2\, C_p - 3\, P_2}{r_2\, T_2\, C_p - P_2}\right)\right] + \sqrt{\left[\frac{V_m}{2}\left(\frac{2\, r_2\, T_2\, C_p - 3\, P_2}{r_2\, T_2\, C_p - P_2}\right)\right]^2 + 4\left[\left(\frac{2\, T_2\, C_p + V_m^{\,2}}{r_2\, T_2\, C_p - P_2}\right)\frac{P_2}{2}\right]}}{2}$$

$$P_3 = \frac{P_2}{T_2\, V_{sr}}\left[T_2 - \frac{V_s^{\,2} - \left(V_s + V_m\right)^2}{2\, C_p}\right]\left(V_s + V_m\right)$$

$$T_3 = T_2 - \frac{V_s^{\,2} - \left(V_s + V_m\right)^2}{2\, C_p}$$

These equations predict a reflection shock speed of 554 m/s, a reflected shock pressure of 0.379 MPa, and a reflected shock temperature of 910 K.

The IFCI calculation of the shock wave is shown in Figure 4 (pressure) and Figure 5 (temperature). The initial shock is shown for times of 0.2, 0.4, 0.6, and 0.8 ms. The reflected shock is shown for times of 1, 1.2, 1.4, and 1.6 ms. Both pressures and temperatures correspond well to the closed form calculations.

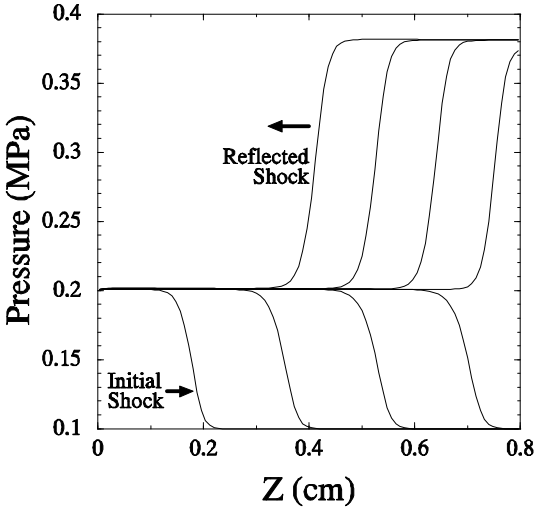

Figure 4 Propagation of Shock and Reflection in Water

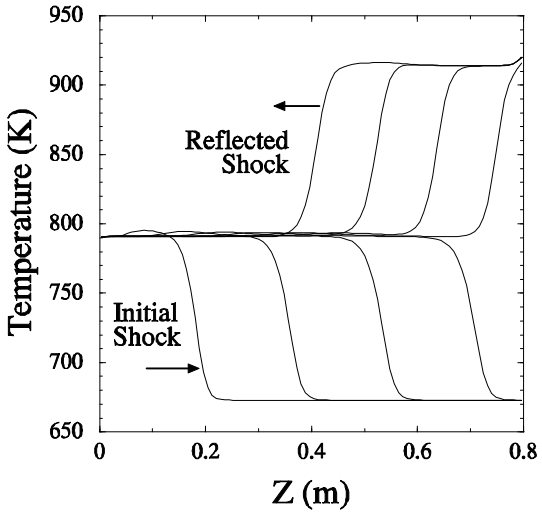

Figure 5 Temperature of Steam in Propagating Shock

The shock front positions are shown in Figure 6 for the propagating shock (0.18 MPa) and the reflected shock (0.36 MPa). The front velocities calculated from this graph are 863 m/s for the initial shock and 570 m/s for the reflected shock. These correspond well to the predicted values.

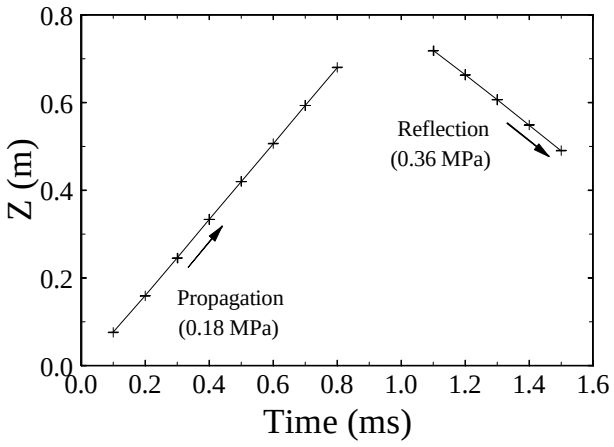

Figure 6 Position of Isobar as a Function of Time (Steam Shock)

4. Shock Propagation in a Two-Phase Mixture

To complete the benchmarking of shock behavior, the case of a shock propagating through a 10 vol% steam 2-phase mixture was calculated. The derivation of a closed form solution requires that several approximations be made. The continuity and momentum equations are written assuming that the material velocity of the steam and the water in the shocked zone are the same, pressure is the same for both phases, and condensation is ignored.

$$r_{v1}\, a_1\, V_1 = r_{v2}\, a_2\, V_2$$

$$r_{\ell 1}\,(1-a_1)V_1 = r_{\ell 2}\,(1-a_2)V_2$$

$$P_1 - P_2 = \left[r_{v1}\, a_1 + r_{\ell 1}\,(1-a_1)\right]V_1(V_2 - V_1)$$

Kinetic energy can be ignored in the energy equation. This means that the water temperature will remain constant across the shock front. However, the steam will initially heat up because of adiabatic compression. If the heat transfer between the steam bubbles and the water is sufficiently slow, the steam temperature will remain at the temperature predicted by adiabatic compression. Only the equation of state for steam (assumed ideal) is needed for closure.

The shock velocity (V_s) for the assumed conditions is predicted by the equation:

$$V_s = \sqrt{\frac{P_1 - P_2}{\left[r_{v1}\, a_1 + r_{\ell 1}(1-a_1)\right]\left[a_1\left(\frac{P_1}{P_2}\right)^{\frac{1}{g}} - 1 + (1-a_1)\frac{r_{\ell 1}}{r_{\ell 2}}\right]}}$$

where g is the isentropic expansion coefficient (~1.3). The equations for the material velocity (V_m), the volume fraction in the shock (a_2), and the shock temperature (T_2) are:

$$V_m = \frac{P_2 - P_1}{\left[r_{v1}\, a_1 + r_{\ell 1}\left(1 - a_1\right)\right] V_s}$$

$$a_2 = \frac{1}{\left(V_s - V_m\right)}\left[\frac{P_1 - P_2}{\left[r_{v1}\, a_1 + r_{\ell 1}\left(1 - a_1\right)\right] V_s} + V_s\left[1 - \left(1 - a_1\right)\frac{r_{\ell 1}}{r_{\ell 2}}\right]\right]$$

$$T_2 = \frac{P_2}{P_1}\frac{a_2}{a_1}\frac{V_s - V_m}{V_s} T_1$$

For this benchmark, the initial and shock pressures were chosen to be 0.1 and 0.3 MPa, respectively. For this condition, the shock velocity, material velocity, and shock volume fraction were predicted to be 63.7 m/s, 3.64 m/s, and 0.04555, respectively. The gas temperature in the shock is predicted to be 481 K. The values calculated on the basis of the low heat transfer assumption were used as the inflow conditions in the IFCI calculation.

As was seen in the gas shock, the material velocity behind the reflected shock must equal zero. This provides closure for the equation set for the reflections. The pressure behind the reflection (P_3) is the solution to the transcendental equation:

$$P_3 - P_2 = \left[r_{v2}\, a_2 + r_{\ell 2}\left(1 - a_2\right)\right]\left[\frac{a_2 + \left(\frac{P_3}{P_2}\right)^{\frac{1}{g}}\left(1 - a_2\right)\frac{r_{\ell 2}}{r_{\ell 3}}}{\left(\frac{P_3}{P_2}\right)^{\frac{1}{g}} - \left[a_2 + \left(\frac{P_3}{P_2}\right)^{\frac{1}{g}}\left(1 - a_2\right)\frac{r_{\ell 2}}{r_{\ell 3}}\right]} + 1\right] V_m{}^2$$

where V_m is the material speed behind the original shock propagation. The equations for the reflection shock speed, gas volume fraction, and temperature are:

$$V_{sr} = V_m \frac{a_2 + \left(\frac{P_3}{P_2}\right)^{\frac{1}{g}}\left(1 - a_2\right)\frac{r_{\ell 2}}{r_{\ell 3}}}{\left(\frac{P_3}{P_2}\right)^{\frac{1}{g}} - \left[a_2 + \left(\frac{P_3}{P_2}\right)^{\frac{1}{g}}\left(1 - a_2\right)\frac{r_{\ell 2}}{r_{\ell 3}}\right]}$$

Error! Not a valid embedded object.

$$T_3 = \left(\frac{P_3}{P_2}\right)^{1-\frac{1}{g}} T_2$$

These equations produce values of 0.798 MPa, 146 m/s, 0.022, and 602 K, for the pressure, velocity, volume fraction, and temperature of the reflected shock.

Figure 7 shows the propagation of the shock into the 2-phase mixture as predicted by IFCI. Pressure profiles of the propagating shock are shown at 2 ms intervals to 12 ms. The reflected wave, which is traveling faster, is shown at times of 14.5, 15, 15.5, 16 ms. Both shock waves propagate consistently, maintaining a constant shock pressure throughout the transit. The pressure values predicted by IFCI are consistent with the closed form predictions.

Figure 8 shows the location of the shock front as predicted by IFCI. Pressure levels of 0.25 and 0.7 MPa were used to define the locations of the propagating and reflecting shocks. Based upon this, propagation and reflection speeds of 61 and 157 m/s were deduced from the IFCI calculation. These are in good agreement with the closed form solutions.

Figure 9 shows the steam temperature in the shock as predicted by IFCI. Figure 10 shows the predicted volume fractions in the shock. The closed form predictions are indicated in both graphs by dotted horizontal lines. Both graphs show the same level of agreement seen in the pressure plot (Figure 7).

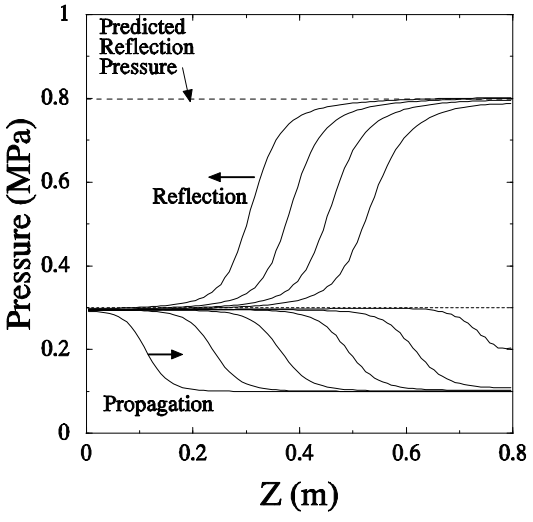

Figure 7 Propagation of Shock and Reflection in a 2-Phase Mixture

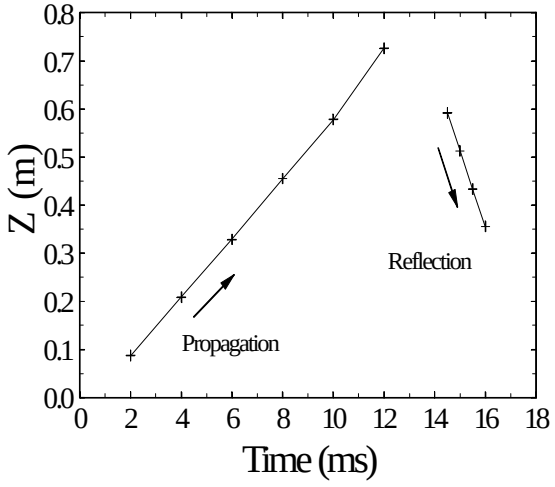

Figure 8 Shock Front Propagation as Deduced from IFCI Calculation

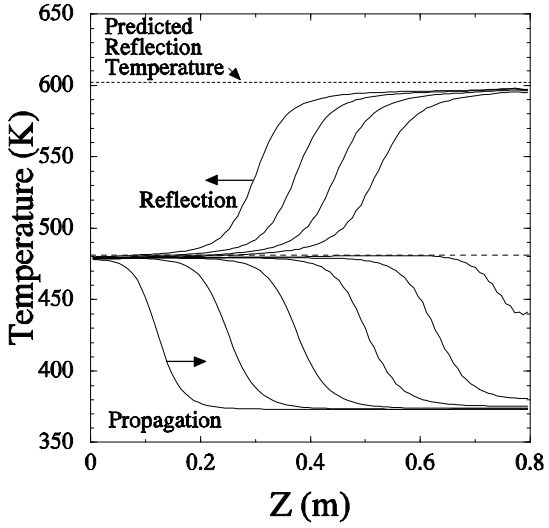

Figure 9 Steam Temperatures in 2-Phase Shock

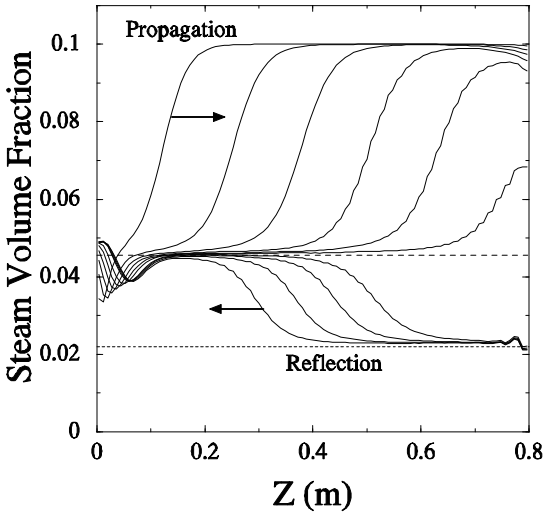

Figure 10 Steam Volume Fractions in 2-Phase Shock

5. Conclusions

All three shock benchmarks show good agreement between the closed-form solutions and the IFCI calculations. From this, it may be concluded that IFCI is capable of correctly calculating shock behavior. The benchmarking process generated one modification to the IFCI code: the addition of artificial viscosity to the shock calculation. This term minimizes numerically-induced pressure oscillations that are produced by the differencing scheme. An brief description of the implementation of artificial viscosity is included in this report as an appendix. It remains to be determined if the value of the artificial viscosity will be included as a user-defined input parameter or will remain as an immutable constant within the code.

During the benchmarking process, it was noted that there is some variation in the values for steam enthalpy in the literature. In IFCI (and TRAC), the values based upon the ASME Steam Tables (4), which appear to extend to 1073 K. The enthalpy of steam above this temperature, as predicted by IFCI, appears to be approximately linear with temperature (Figure 11). However, the steam enthalpy values published by the National Bureau of Standards [2] show a more nonlinear behavior at higher temperatures. This appears to be due to the inclusion of rotational modes in the internal energy calculation. The difference between the two curves may have an impact on the fine fragmentation portion of the FCI. It is likely that this possibility will need to be addressed at

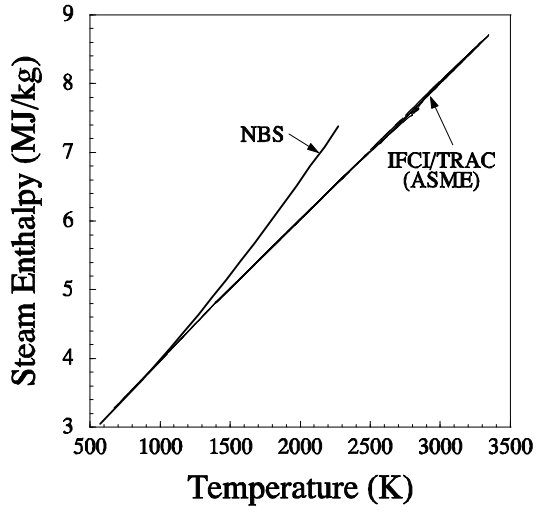

Figure 11 Steam Enthalpy Values from ASME and NBS

some time in the future.

APPENDIX: Notes on Artificial Viscosity in IFCI

During testing of the shock calculations in IFCI, it was noted that oscillations developed behind the shock front in water, and in the reflected shock in steam vapor. These oscillations were persistent, indicating insufficient dissipation. It was decided to try artificial viscosity to increase dissipation.

The form chosen is that of an artificial viscous pressure, which minimizes changes to the existing code structure; the viscous pressure is simply added to the pressure in the momentum and energy equations. The viscous pressure is of the form

$$q_k = \begin{cases} -v_s \Delta x r_k D_k & D_k < 0 \\ 0 & D_k \geq 0 \end{cases}$$

where

q_k = artificial viscous pressure to be added to equations for field k,
v_s = viscous coefficient determined by numerical experiment,
Dx = average of radial and axial cell dimensions,
r_k = density of field k,
D_k = divergence of field k.

The divergence for field k is defined in cylindrical coordinates as

$$D_k = \frac{\partial v_k}{\partial z} + \frac{\partial u_k}{\partial r} + \frac{u_k}{r}$$

In finite difference form, this was implemented as

$$D_{kj,i} = \frac{v_{kj,i} - v_{kj-1,i}}{\Delta z_j} + \frac{u_{kj,i} - u_{kj,i-1}}{\Delta r_i} + \frac{u_{kj,i} + u_{kj,i-1}}{2 r_i}$$

where index j,i refers to axial level j, radial ring i.

REFERENCES

1 R. H. Sabersky, et. al., Fluid Flow, A First Course in Fluid Mechanics, 2nd ed., The Macmillan Company, New York (1971).

2 J. S. Gallagher (National Bureau of Standards) and George S. Kell (National Research Council of Canada), NBS/NRC Steam Tables: Thermodynamic and Transport Properties and Computer Programs for Vapor and Liquid States of Water in SI Units, Hemisphere Publishing Corporation, New York (1984).

3 D. R. Liles, et. al., TRAC-PFI/MOD1 Correlations and Models, NUREG/CR-5069, LA-11208-MS, Los Alamos National Laboratory (1988).

4 ASME Steam Tables: Thermodynamic and Transport Properties of Steam, 5th ed. The American Society of Mechanical Engineers, New York (1983).